Investigations of the Thermal, Structural, and Near-IR Emission Properties of Ag Containing Fluorophosphate Glasses and their Crystallization Process

Marwa Ennouri[1], Laeticia Petit[2], and Habib Elhouichet[3,1,*]

[1] Laboratoire de Caractérisations, Applications et Modélisation des Matériaux LR18ES08, Sciences Faculty of Tunis, University of Tunis El Manar 2092, Tunisia.

[2] Photonics Laboratory, Tampere University, FI-33101 Tampere, Finland.

[3] Physics department, College of Sciences, University of Bisha, P.B. 551, Bisha 61922, Saudi Arabia.

*Corresponding author: habib.elhouichet@fst.rnu.tn

Abstract

In this work, the impact of Ag_2O on the thermal, structural, and Near-IR luminescence of Er^{3+} doped calcium-fluorophosphate glasses is investigated. The amount of silver oxide in the glass significantly impacts its thermal stability and crystallization process. The increase in the thermal stability of the glasses might be attributed to the depolymerization of the metaphosphate network evidenced using FTIR and Raman spectroscopies. The precipitation of Ag nanoparticles within the glass network, induced by a thermal treatment, has been confirmed by the appearance of a clear visible broad absorption band centered at about 450 nm in the glasses after heat treatment. Such species induce a significant enhancement in the Er^{3+} IR emission. Transparent glass-ceramics have also been processed by thermally treating the glasses. The XRD analyses have revealed that the addition of Ag_2O in the glass promotes the precipitation of new crystalline phases at the expense of CaF_2 crystals. The presence of such nanostructures in the glass network induces some modifications in the distribution of Er ion sites.

Introduction

Rare-earth (RE) doped glasses have been in the limelight over the last decades as they provide adequate answers to the technological challenges of several photonic applications in telecommunications, information storage, solar cells, light detection, and bio-imaging [1] [2] [3] [4] [5]. Impressively, RE active ions possess interesting spectral features as well as a variety of attractive emissions ranging from the visible to the IR range. Among them, Erbium (Er^{3+}) presents a particularly broad emission at around 1.53 μm, corresponding to the lowest-loss optical communication window. Nevertheless, the development of highly luminescent glasses using Er^{3+} ions imposes a thoughtful choice of the vitreous matrix. In this context, fluoro-phosphate-based glasses have received a great interest due to their combined merits of phosphate and fluoride glass hosts [6][7][8]. Under phosphate chains, the host could possess excellent transparency, good thermal and mechanical stability, high solubility of active ions, and low melting points [9] [10]. The addition of fluorine compounds in the main phosphate host firstly decreases its phonon energy, red-shift its IR cutoff edge and increases then its ability as a fiber amplifier host. The presence of fluorine compounds could also play a valuable part in the reduction of OH^- groups, which limits the RE non-radiative losses [11] [12].

Within the goal of tailoring the optical and spectroscopic features of Er^{3+} ion in these promising hosts, several ways can be adopted. Of late, linking RE ions with metallic Ag nanostructures has been demonstrated to efficiently enhance the RE ions luminescence mainly through controlling the excitation transfers [13] [14] [15]. Ag species are known to have promising non-linear optical properties either as isolated Ag^+ ions, Molecule-like nanoclusters (NCs) Ag_m^{n+}, or also as plasmonic nanoparticles (NPs). These species are capable to ensure a resonant energy transfer to RE ions improving the pumping efficiency and, therefore, the emission properties [16]. The particular relevance of these species stems from their plasmonic effect [17]. The collective oscillation of conduction electrons produced at the surface of the nanoparticle generates a high localized electromagnetic field, which, in turn, dramatically increases the RE transition probabilities, enhancing their spectral features. This phenomenon is known as local field enhancement (LFE) by surface Plasmon resonance (SPR) of Ag NPs [18][19]. Moreover, as nanoparticles, Ag can intervene to absorb the hydroxyl groups and suppress the deleterious energy losses [20].

The improvement of lanthanides (Ln^{3+}) luminescence may also be achieved by tailoring their local site symmetry and intensifying their surrounding crystal field. This can be achieved by the creation of nanosized crystal structures within the vitreous host. For instance, the

incorporation of Ln^{3+} ions in fluoride nanostructures was found to promote a high site regularity and a low phonon frequency without altering the advantages of the glass host [21] [22]. This technology offers attractive luminescence characteristics for the active ions such as increased radiative transition probabilities, long luminescence lifetimes and good quantum yields [22] [23]. Thus, it is interesting to induce further processes of excitation transfer to rare eath ions from Ag species and nanocrystals embedded in the glassy host.

Although several studies on Ag-containing Er-doped glasses are available in the literature [24] [25] [26], only a few have investigated the impact of Ag on the crystallization process of the glasses, which is fundamental to show the ability of glass-ceramic formation and thus designing improved optical materials.

In this paper, we report the thermal, structural, and Near-IR emission features of Er^{3+} embedded in new calcium-fluorophosphate glasses in the presence of Ag species. The impact of Ag_2O on the crystallization processes of glasses will be also discussed, in an effort to develop efficient Near-IR glass-ceramic fibers.

Experimental methods

Calcium-fluorophosphate glasses within the composition (100-x) ($0.7276NaPO_3$- $0.0249ZnO$- $0.2425CaF_2$)- xAg_2O- $0.5Er_2O_3$ (in mol%), were elaborated via the classic melt-quenching process under different Ag_2O concentrations (x= 0, 0.5, 1, and 4 mol%). 15 g batches of $(NaPO_3)_6$ (Alfa Aesar, 99.99%), ZnO (Sigma Aldrich, ≥99.5%), Ag_2SO_4 (Sigma Aldrich, 99.99%), and Er_2O_3 (MV Laboratories Inc, 99.5%) were mixed and placed in an alumina crucible in which they were melted for only 5 min at 1020°C to avoid fluorine losses during synthesis [27],[28]. The molten liquid was then thoroughly mixed and poured into a brass plate to obtain a glass. Finally, a post-annealing of 4h at 200°C was carried out on the resulted glasses to minimize the mechanical stress produced during the synthesis.

The density of the glasses was measured with an accuracy of ± 0.02 gcm^{-3} from bulk samples by Archimede's method, where ethanol was the immersion fluid.

Differential thermal analyses (DTA) were performed on glass powder by using STA 449 Netzsch F1 equipment, under N_2 atmosphere. The data were collected from 50 to 550 °C at 10 °C min^{-1}. From DTA curves, the characteristic temperatures of the glasses, such as the glass transition temperature (T_g), the onset crystallization temperature (T_x), and the crystallization temperature (T_p) were determined respectively, as the inflection point of the first

endothermic event, the onset, and the maximum of the exothermic event. The temperatures are given at ± 3ºC.

The nature of the crystals precipitated during the thermal treatment was obtained from X-ray diffraction (XRD) analysis. The XRD patterns were collected using the Panalytical EMPYREAN multipurpose Diffractometer using *Cu-Kα* radiation (λ = 1.54056 Å).

Attenuated Total Reflection FTIR Perkin Elmer Spectrophotometer was used to measure the IR absorption spectra of the glasses. The measurement was performed on powdered samples in the range 650–1500 cm^{-1} within a resolution of 2 cm^{-1}.

Polished samples were used to collect the Raman spectra of the glasses within the range 600-1400 cm^{-1}. The measurements were performed by inVia Qontorfi confocal Raman microscope with a laser excitation of 405 nm.

The UV-Vis-NIR absorption spectra of the as-prepared glasses were collected via a Perkin Elmer Lambda 900 UV-Vis-NIR spectrometer with an integrating sphere setup, in the spectral range 250-2000 nm. Data with a resolution of 0.2 nm were collected from polished samples of almost 2 mm thickness. The absorption cross-sections $\sigma_a(\lambda)$ of the glasses were obtained from the experimental data by:

$$\sigma_a(\lambda) = \frac{log10}{N\,d}\,A(\lambda) \qquad (1)$$

Where $A(\boldsymbol{\lambda})$ represents the absorbance at $\boldsymbol{\lambda}$, N is the number of Er^{3+} ions in cm^3, and d is the sample thickness.

Jobin Yvon iHR320 spectrometer instrument was used to record the IR emission spectra from bulk samples of almost the same thickness, under excitation of 980 nm. A Thorlabs FEL 1500 filter and a Hamamatsu P4631-02 detector were used. The samples were excited with a single-mode monochromatic fiber laser diode. The accuracy of the measurement was about 10%.

Results and discussions

Table 1 displays the density and the thermal parameters of the studied glasses. As seen, an increase in the Ag concentration increases the density of the glasses. This behavior is mostly owed to the higher molecular weight of Ag_2O content compared to those relative to their substituted elements, $NaPO_3$, ZnO, and CaF_2 [29]. In addition, as x increases, each of T_g, T_x,

and T_p increase, resulting in an increased width of the supercooled liquid region. The appearance of new exothermic events seen in the DTA curves (Fig.1) could be attributed to preferential surface crystallization of the glass. Based on previous studies [30] [31], the presence of metallic silver ions contributes to the creation of new heterogeneous nucleation sites, reducing the rates of diffusion of the major crystal phases.

To get more insight into the different thermal features of the glasses, the structural modifications induced by Ag_2O addition were investigated via FTIR and Raman spectra (Fig. 2). All the FTIR spectra are normalized to the band located at about 1100 cm^{-1}. The IR spectra (Fig. 2 (a)) display the same bands at ~730, 890, 1100, and 1260 cm^{-1} and shoulders at around 970, 1015, and 1085 cm^{-1} for all the investigated glasses. The bands located at 730, 890, and 1260 cm^{-1} are assigned respectively, to the stretching vibrations υ_{ss}(POP), υ_{as}(POP), and υ_{as}(OPO) of Q^2 groups [32] [33]. The features at 970 and 1085 cm^{-1} are attributed to the fundamental vibrations $\upsilon_{as}(PO_3^{2-})$ and $\upsilon_{ss}(PO_3^{2-})$ in Q^1 groups, respectively [32] [33]. As previously suggested, the shoulder founded at 1015 cm^{-1} is characteristic of symmetric vibrations of PO_3F^{2-} groups [34]. Similar IR absorption spectra were reported in the work of S. Cui et al. [35], where a detailed analysis with band assignments can be found. From the foregoing, the structure of the investigated glasses builts around metaphosphate tetrahedra (Q^2) with pyrophosphate (Q^1) and monofluoro-prthophosphate (PO_3F) species. The decrease in the intensity of the bands at 730, 890, and 1260 cm^{-1} and of the shoulders at 970 and 1015 cm^{-1} with the shift of the main band to lower wavenumbers, when x increases from 0 to 1 mol%, indicates the formation of a greater number of Q^1 groups at the expense of Q^2 groups. In agreement with the thermal results, the addition of silver oxide in small quantities might cause a depolymerization of the phosphate network.

The Raman spectra of the investigated glasses were normalized at the high-intensity band and displayed in Fig. 2 (b). The band attributions were reported in detail in ref [35]. The band centered at around 700 cm^{-1} might be linked to symmetric stretching modes (υ_{ss}(POP)) of bridging oxygens in metaphosphate tetrahedra. The bands at ~1150 and 1260 cm^{-1} are originated from the symmetric and asymmetric vibration modes of non-bridging oxygens in Q^2 species, $\upsilon_{ss}(PO_2)$ and $\upsilon_{as}(PO_2)$, respectively. In addition, the small band that appears around 910 cm^{-1} is probably due to the asymmetric vibration modes of NBOs in isolated Q^0 groups [36]. Consistent with FTIR analysis, the addition of silver oxide in the glass influences the P-O bridging and thus the Q^n units. An increase in x from 0 to 4 mol% leads to a progressive shift to lower wavenumbers of the band at 1150 cm^{-1} and to higher wavenumbers of the band at 700

cm^{-1} accompanied by a decrease in the intensity of the band at 1025 cm^{-1}. This reveals a shortening in the metaphosphate chains, confirming the depolymerization of the phosphate network and the development of higher number of NBOs. Similar tendency was previously reported in the work of Kuusela et al. [37] when adding ZnO to sodium fluorophosphate glasses.

Fig. 3 depicts the absorption (a) and emission (b) spectra of the investigated glasses. The absorption spectra (Fig. 3 (a)) exhibit several absorption bands originating from the 4f-4f transitions typical of Er^{3+}-doped glassy hosts, from the ground level ($^4I_{15/2}$) to their respective upper levels. As shown in Fig. 3 (a), an increase in Ag_2O content leads to a continuous shift in the UV-absorption edge towards lower frequencies. According to the structural changes, as x increases from 0 to 4 mol %, Ag_2O leads to a more depolymerized structure with a greater number of NBOs reducing the bandgap energy. The red-shift of the bandgap in the presence of Ag species can be also explained by the fact that the electrons of Ag^+ elements (with the electronic configuration d^{10}) contribute to the valence band tailing and thus diminish the badgap energy when x increases [37] [38]. No surface plasmon resonance band from Ag nanoparticles can be seen in the absorption spectra indicating that the Ag atoms are in ionic form in the glass. Considering the accuracy of the measurements, the absorption coefficients and cross-sections at 1.53 µm (Table 1) are almost the same for all the glasses, which means that the Er^{3+} ion sites were not strongly affected by the addition of Ag_2O. The absorption cross-section of the glasses are similar to those reported in phosphate glasses [39].

The emission spectra presented in Fig. 3 (b) show the typical Near-IR feature of Er^{3+} ion corresponding to the $^4I_{13/2} \rightarrow {}^4I_{15/2}$ transition. One notices that the emission intensity slightly decreases when Ag concentration increases from 0 to 4 mol%. Such behavior might be explained by considering the number of Er^{3+} ions /cm^3 (Table 1). We assume that the increase in Er^{3+} ions/cm^3 leads to a shorter Er-Er distance, which increases the clustering rate of Er^{3+} ions decreasinf slightly the intensity of the emission. Based on the structural properties of the glasses, the depolymerization of the phosphate network is suspected to diminish the distance between RE ions, which corresponds to an increase in their clustering, as previously suggested by P. Goldner et al. [40]. The change in the shape of the Er^{3+} emission band indicates slight modifications in the Er^{3+} ions sites when adding Ag_2O.

Within the goal of precipitating Ag NPs in the glass, the as-prepared samples were optically polished and thermally treated slightly above their transition temperatures ($T_g+10°C$) for 2, 4, and 17h [41]. In addition to the absorption features of Er^{3+} ions, the absorption spectra

of the thermally treated glasses (Fig. 4) show the appearance of new broad absorption centered at ~ 450 nm overlapping with the RE absorption bands. As reported by ref [42] [43], such absorption is linked to the surface plasmon resonance (SPR) band of Ag NPs. As resume in Fig. 4 (d), the Ag NPs absorption band seems to be more pronounced for short heat-treatment durations. Moreover, increasing the duration of the thermal treatment from 2 to 4h, the Ag NPs absorption band slightly shifts to higher wavelengths. These spectral changes could be related to the formation of larger size particles by increasing both the Ag precursor concentration and the thermal treatment duration. As previously demonstrated [44] [45], small Ag nanoparticles are characterized by intense light absorption, while larger nanoparticles may exhibit high scattering of light, evidenced by the broadening and redshifting of the SPR band. On the other hand, a heat-treatment of the glasses for 17h leads to a high scattering of light. That seems to be due to the precipitation of some crystalline phases at the glass surface.

One should mention that the precipitation of the Ag NPs occurs only at the surface of the glasses as in [46]. After polishing the heat-treated glasses, the SPR band disappear in the absorption spectrum of all the glasses.

Narrow diffraction peaks can be seen only in the XRD pattern of the heat-treated Ag4 glass (Fig. 5) and they can be related to Ag_3PO_4 crystalline phase according to the JCPDS card No. 01- 074-1876. Here, the glass structure is still dominated by the amorphous character, as supported by the weakness of the intensity of the crystalline peaks compared to that of the amorphous hump [23]. The latter results should significantly influence the emission features of the glasses. As the shape of the emission band presented in Fig. 6 remains broad without the appearance of sharp peak after the thermal treatment, the Er^{3+} ions are suspected to remain in the amorphous part of the glass. The bandwtdh of the emission band decreases after heat treatment of the Ag4 glass probably due to the precipitation of Ag_3PO_4 which is suspected to reduce the site distribution of the Er^{3+} ions. As seen from Fig. 6 (d), a great improvement in the NIR emission was obtained for almost all the heat-treated samples due to the local field enhancement induced by SPR of metal NPs and the resonant energy transfer from Ag NPs to Er^{3+} ions. These two mechanisms seem little probable as they require an overlapping between the energy levels of the NP and those of the active ions [15]. M. Fukushima et al. [20] suggested that the enhancement of the Er^{3+} luminescence at 1.53 µm when exciting at 980 nm can be originated from chemical effects, as Ag NPs may act as hydroxyl group absorbers, reducing the Er^{3+} non-radiative losses, increasing thus their emission intensity. The decrease in the Er^{3+} emission intensity for almost all the heat-treated samples for 17h can be to the large amount of

Ag species precipating in the glasses leading to energy transfer from the exited states of Er^{3+} to the silver NPs, as suggested in [47] and/or to the surface crystallization which might decrese the Er-Er distance in the glass.

In order to grow crystals in the glasses, the as-prepared glasses were heat-treated firstly at their respective $T_g+20\ °C$ for 17h and then at T_p for 1 h [35] [39]. Fig. 7 shows the appearance of the obtained samples prior to and after polishing. Independently of the Ag_2O amount, all the glasses look completely opaque after the thermal treatment which is a clear sign of surface crystallization. Fig.8 (a) shows the XRD spectra taken from the surface of the heat-treated samples prior to polishing. The peaks present in the sample with x=0 are mostly related to CaF_2 (ICDD PDF#00-004-0864), $Ca(PO_3)_2$ (ICDD PDF#00-011-0039), and $Ca_3(PO_4)_2$ (ICDD PDF#00-006-0426). The increase in Ag amount decreases the intensity of the peaks related to CaF_2 crystals and new peaks which can be related to $Ca_5(PO_4)_3F$ (ICDD PDF#01-071-0880) crystalline phase appear after the thermal treatment. Peaks related to Ag (ICDD PDF#00-001-1167) crystals are also clearly visible in the XRD of the Ag4 glass after heat treatment. Fig. 8 (b) presents the XRD patterns of the heat-treated glasses after polishing. The XRD pattern of the Ag-free glass show the formation of a single CaF_2 (ICDD PDF#00-004-0864) crystalline phase the thermal treatment whereas, no peaks can be seen in the XRD of the Ag-containing glasses confirming their amorphous character after heat treatment. Thus, the progressive addition of Ag_2O limits the precipitation of CaF_2 crystals. That can be explained by the distortion of the glass chain, as evidenced by FTIR and Raman spectroscopies. In agreement with [39], the thermal treatment has no impact on the intensity of the emission at 1.5µm. However, the shape of the emission band at 1.53 µm (Fig. 9) undergone some changes after the thermal treatment. As seen, the emission band of the Ag0 glass-ceramic sample is the only emission band exhibiting a more resolved structure when referring to the Stark splitting that appears at about 1505 nm, indicating the incorporation of Er^{3+} ions in a more intensified local field environment. Similar changes in the emission spectra due to the precipitation of CaF2 crystals were reported in [36]. One can notice that the bandwidth of the emission from the Ag containing glasses decreases after the thermal treatment indicating that the thermal treatment decreases the Er^{3+} site distribution.

Conclusion

Highly luminescent glasses within the compositions (100-x)(0.7276$NaPO_3$-0.0249ZnO- 0.2425CaF_2)-xAg_2O -0.5Er_2O_3 were successfully elaborated via classic melt-quenching process. The amount of silver oxide in the glass has an appreciable influence on its crystallization process. Based on the analysis of the FTIR and Raman spectra, the addition of Ag_2O leads to the depolymerization of the metaphosphate network, as supported by the reduction of the optical bandgap. The precipitation of Ag nanoparticles at the surface of the glasses has been confirmed by the appearance of a clear broad absorption band at about 450 nm after the thermal treatment. Such species induce a significant enhancement in the Er^{3+} IR emission. Transparent glass-ceramics were also prepared by thermally treating the glasses at their respective nucleation temperature (T_g+*20°C*) and then at T_p for 1 hour.The impact of the glass composition on the nucleation and the growth process was investigated via XRD analysis. It is found that the progressive addition of Ag_2O in the glass network promotes, during the thermal treatment, the development of new heterogeneous nucleation sites, limiting the precipitation of CaF_2 crystalline phases.

Acknowledgements

LP would like to acknowledge Academy of Finland (Flagship Programme, Photonics Research and Innovation PREIN-320165 and Academy Project -326418) for the financial support.

References

[1] R. Reisfeld, Future technological applications of rare-earth-doped materials, *J. Common Met.* 93 *(1983) 243-251*.

[2] A. B. Seddon, Z. Tang, D. Furniss, S. Sujecki, T. M. Benson, Progress in rare-earth-doped mid-infrared fiber lasers, *Opt. Express*. 18 (2010) 26704-26719.

[3] C. W. Thiel, T. Böttger, R. L. Cone, Rare-earth-doped materials for applications in quantum information storage and signal processing , *J. Lumin.* 131 (2011) 353-361.

[4] L. de A. Florêncio, L. A. Gómez-Malagón, B. C. Lima, A. S. L. Gomes, J. A. M. Garcia, L. R. P. Kassab, Efficiency enhancement in solar cells using photon down-conversion in Tb/Yb-doped tellurite glass, *Sol. Energy Mater. Sol. Cells*. 157 (2016) 468-475.

[5] J. Zhong, D. Chen,Y. Peng, Y. Lu, X. Chen, X. Li, Z. Ji, A review on nanostructured glass ceramics for promising application in optical thermometry, *J. Alloys Compd.* 763 (2018) 34-48.

[6] M. Ennouri, I. Jlassi, H. Elhouichet, Luminescence improvement of Sm^{3+} doped fluoro-phosphate glass by silver species, *J. Non-Cryst. Solids* 551 (2021) 120397.

[7] I. Jlassi, S. Mnasri, H. Elhouichet - Concentration dependent spectroscopic behavior of Sm^{3+}-doped sodium fluoro-phosphates glasses for orange and reddish-orange light emitting applications, *J. Lumin. 199 (2018) 516–527*.

[8] M. Ennouri, L. Kuusela, I. Jlassi, B. Gelloz, L. Petit, Habib Elhouichet, Impact of the Ag_2O Content on the Optical and Spectroscopic Properties of Fluoro-Phosphate Glasses, *Materials 12 (2019) 3516*.

[9] M. Saad, H. Elhouichet, Good optical performances of Eu^{3+}/ Dy^{3+} /Ag nanoparticles co-doped phosphate glasses induced by plasmonic effects, *J. Alloys Compds 806 (2019) 1403*.

[10] P. Stoch, A. Stoch, M. Ciecinska, I. Krakowiak, M. Sitarz, Structure of phosphate and iron-phosphate glasses by DFT calculations and FTIR/Raman spectroscopy, *J. Non-Cryst. Solids*. 450 (2016) 48-60.

[11] E. Kolobkova, A. Alkhlef, B.M. Dinh, A.S.Yasukevich, O.P. Dernovich, N.V. Kuleshov, N. Nikonorov, Spectral properties of Nd^{3+} ions in the new fluoride glasses with small additives of the phosphates, *J. Lumin.* 206 (2019) 523-529.

[12] J. Lucas, Fluoride glasses, *J. Mater. Sci*. 24 (1989) 1-13.

[13] H. Fares, H. Elhouichet, B. Gelloz, M. Férid, Silver nanoparticles enhanced luminescence properties of Er^{3+} doped tellurite glasses: Effect of heat treatment. *J. Appl. Phys. 116* (2014) 123504:1–123504:10, doi:10.1063/1.4896363.

[14] R. J. Amjad, M.R. Dousti, M.R.Sahar, Spectroscopic investigation and Judd–Ofelt analysis of silver nanoparticles embedded Er^{3+}-doped tellurite glass, *Curr. Appl. Phys*. 15 (2015) 1-7.

[15] M. Ennouri, B. Gelloz, H. Elhouichet, Impact of Ag species on luminescence and spectroscopic properties of Eu^{3+} doped fluoro-phosphate glasses, *J. Non-Cryst. Solids*. 570 (2021) 120938.

[16] R. F. Wei, J. Li, J. Gao, H. Guo, Enhancement of Eu^{3+} Luminescence by Ag Species (Ag NPs, ML-Ag, Ag^{+}) in Oxyfluoride Glasses, *J. Am. Ceram. Soc. 95 (2012) 3380-3382*.

[17] F. Gonella, Silver doping of glasses, *Ceram. Int.*. 41 *(2015) 6693-6701*.

[18] M. Moskovits, Surface-enhanced spectroscopy, *Rev. Mod. Phys.* 57 (1985) 783-826.

[19] M. Saad, W. Stambouli, S. A. Mohamed, H. Elhouichet, Ag nanoparticles induced luminescence enhancement of Eu^{3+} doped phosphate glasses, *J. Alloys Compd. 705 (2017) 550*.

[20] M. Fukushima, N. Managaki, M. Fujii, H. Yanagi, S. Hayashi, Enhancement of 1.54-μm emission from Er-doped sol-gel SiO_2 films by Au nanoparticles doping, *J. Appl. Phys. 98 (2005) 024316*.

[21] H Fares, W Stambouli, H Elhouichet, B Gelloz, M Férid, Nano-silver enhanced luminescence of Er^{3+} ions embedded in tellurite glass, vitro-ceramic and ceramic: impact of heat treatment, *RSC Advances 6 (2016) 31136-31145*.

[22] G. Lakshminarayana, R. Yang, M. Mao, J. Qiu, et I. V. Kityk, Photoluminescence of Sm^{3+}, Dy^{3+}, and Tm^{3+}-doped transparent glass ceramics containing CaF_2 nanocrystals, *J. Non-Cryst. Solids*. 355 *(2009) 2668-2673*.

[23] M. Ennouri, I. Jlassi, H. Elhouichet, B. Gelloz, Improvement of spectroscopic properties and luminescence of Er^{3+} ions in phospho-tellurite glass ceramics by formation of $ErPO_4$ nanocrystals, *J. Lumin. 216 (2019) 116753*.

[24] C. Strohhöfer, A. Polman, Silver as a sensitizer for erbium, *Appl. Phys. Lett.* 81 (2002) 1414-1416.
[25] I. I. Kindrat, B. V. Padlyak, R. Lisiecki, V. T. Adamiv, I. M. Teslyuk, Enhancement of the Er3+ luminescence in Er–Ag co-doped $Li_2B_4O_7$ glasses, *Opt. Mater.* 85 (2018) 238-245.
[26] E. Trave, M. Back, E. Cattaruzza, F. Gonella, F. Enrichi, T. Cesca, B. Kalinic, C. Scian, V. Bello, C. Maurizio, G. Mattei, Control of silver clustering for broadband Er^{3+} luminescence sensitization in Er and Ag co-implanted silica, *J. Lumin.* 197 (2018)104-111.
[27] A.Szczodra, L. Kuusela, I. Norrbo, A. Mardoukhi, M. Hokka, M.Lastusaari, L. Petit, Successful preparation of fluorine containing glasses with persistent luminescence using the direct doping method, *J. Alloys Compd.* 787 (2019) 1260-1264;
[28] L.A. Bueno, Y. Messaddeq, F.A. Dias Filho, S.J.L. Ribeiro, Study of fluorine losses in oxyfluoride glasses, *J. Non-Cryst. Solids* 351 (2005) 3804-3808
[29] S. Aravindan, V. Rajendran, N. Rajendran, Influence of Ag_2O on crystallisation and structural modifications of phosphate glasses, *Phase Transit. 85 (2012) 630-649*.
[30] S. Banijamali, B. E. Yekta, A. R. Aghaei, The effect of ionic and metallic silver on the crystalline phases developed in CaO–Al_2O_3–TiO_2–P_2O_5 glasses, *J. Non-Cryst. Solids 358 (2012) 303-309*.
[31] M. Reza Dousti, M. R. Sahar, S. K. Ghoshal, R. J. Amjad, A. R. Samavati, Effect of AgCl on spectroscopic properties of erbium doped zinc tellurite glass, *J. Mol. Struct.* 1035 (2013) 6-12.
[32] I. Konidakis, C.-P. E. Varsamis, E. I. Kamitsos, D. Möncke, et D. Ehrt, Structure and Properties of Mixed Strontium−Manganese Metaphosphate Glasses, *J. Phys. Chem. C 114 (2010) 9125–9138*.
[33] M Saad, W Stambouli, N Sdiri, H Elhouichet, Effect of mixed sodium and vanadium on the electric and dielectric properties of zinc phosphate glass, *Mat. Res. Bulletin 89, 224-231 (2017)*.
[34] M. K. Murthy, Phosphate-Halide Systems: II, Infrared Spectra of Glasses in the System NaPO3-NaF, *J. Am. Ceram. Soc. 46 (1963) 558-559*.
[35] S. Cui, J. Massera, M. Lastusaari, L. Hupa, L. Petit, Novel oxyfluorophosphate glasses and glass-ceramics, *J. Non-Cryst. Solids 445-446 (2016) 40-44.*
[36] M.A. Cherbib, I. Khattech, H. Elhouichet, Structure and luminescent properties of Sm^{3+}-doped metaphosphate glasses, *Opt. Mat. 121 (2021) 111571*.
[37] L. Kuusela, A. Veber, N. G. Boetti, L. Petit, Impact of ZnO Addition on Er^{3+} Near-Infrared Emission, the Formation of Ag Nanoparticles, and the Crystallization of Sodium Fluorophosphate Glass, *Materials 13 (2020) 527*.
[38] Y. Hosogi, H. Kato, A. Kudo, Visible light response of $AgLi_1/3M_2/3O_2$ (M = Ti and Sn) synthesized from layered Li_2MO_3 using molten $AgNO_3$, *J. Mater. Chem.* 18 (2008) 647-653.
[39] N. Ojha, A. Szczodra, N. G. Boetti, J. Massera, L. Petit, Nucleation and growth behavior of Er^{3+} doped oxyfluorophosphate glasses, *RSC Advances. 10 (2020) 25703–25716*.
[40] P. Goldner, B. Schaudel, M. Prassas, F. Auzel, Influence of the host structure and doping precursors on rare earth clustering in phosphate glasses analysed by co-operative luminescence, *J. Lumin. 87-89 (2000) 688-690*.
[41] J. Sancho-Parramon, V .Janicki, P. Dubček, M. Karlušić, D. Gracin, M. Jakšić, S. Bernstorff, D. Meljanac, K. Juraić, Optical and structural properties of silver nanoparticles in glass matrix formed by thermal annealing of field assisted film dissolution, *Opt. Mater. 32 (2010) 510-514*.
[42] I. Mechregui H. Fares, S. A. Mohamed, M. Nalin, H. Elhouichet, Coupling between surface plasmon resonance and Sm^{3+} ions induced enhancement of luminescence properties in fluoro-tellurite glasses, *J. Lumin. 190 (2017) 518-524*.
[43] J. A. Jiménez, M. Sendova, H. Liu, F. E. Fernández, Supersaturation-Driven Optical Tuning of Ag Nanocomposite Glasses for Photonics: An In Situ Optical Microspectroscopy Study, *Plasmonics 6 (2011) 399-405*.
[44] T. Kiba, K. Masui, Y. Inomata, A. Furumoto, M. Kawamura,Y. Abe, K.H. Kim., Control of localized surface plasmon resonance of Ag nanoparticles by changing its size and morphology, *Vacuum 192 (2021) 110432*.
[45] W. Wu, M. Wu, Z. Sun, G. Li, Y. Ma, X. Liu, X, Wang, X. Chen, Morphology controllable synthesis of silver nanoparticles: Optical properties study and SERS application, *J. Alloys Compd. 579 (2013) 117–123*.
[46] M. Ennouri, L. Kuusela, I. Jlassi, B. Gelloz, L. Petit, H. Elhouichet, Impact of Ag_2O Content on the Optical and Spectroscopic Properties of Fluoro-Phosphate Glasses, *Materials 12 (2019) 3516*.

[47]H. Fares, H. Elhouichet, B. Gelloz, M. Férid, Surface plasmon resonance induced Er^{3+} photoluminescence enhancement in tellurite glass, *J. Appl. Phys. 117 (2015) 193102*.

Tables

Table 1: Thermal and physical properties of the as-prepared glasses.

Sample	**T_g ± 3°C**	**T_x ± 3°C**	**T_p ±3°C**	**ΔT ± 3°C**	**ρ ± 0.02 g/cm^3**	**N ± 5% (10^{20} ions/cm^3)**	**α at 1.5 µm ±5% (cm^{-1})**	**σ_{Abs} at 1.5 µm (10^{-21} cm^2) ±10%**
Ag0	295	374	490	79	2.71	1.681	0.970	5.77
Ag0.5	307	388	504	81	2.75	1.694	0.969	5.72
Ag1	310	389	509	79	2.78	1.701	0.964	5.67
Ag4	311	391	512	80	2.90	1.704	0.936	5.49

Figures

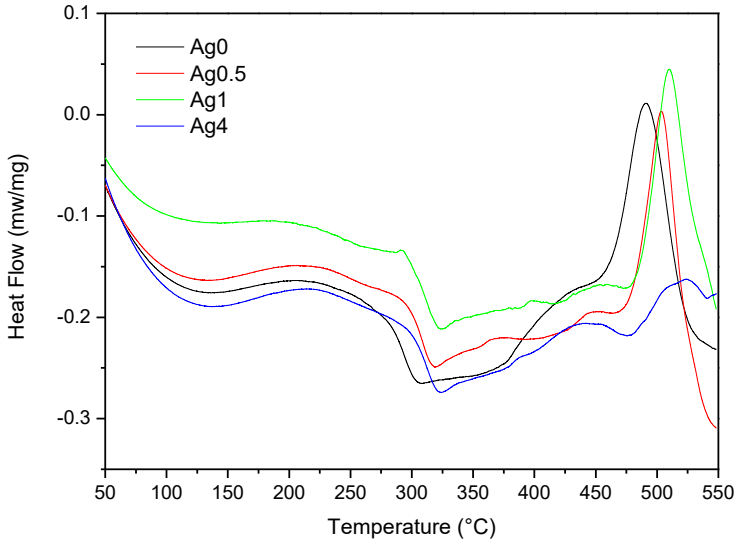

Fig. 1: DTA curves of the as-prepared glasses.

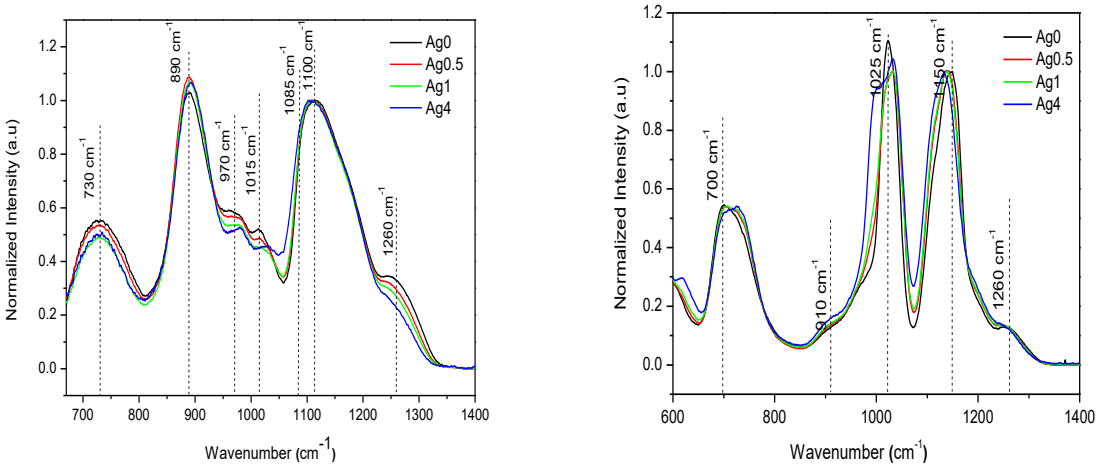

Fig. 2 : (a) FTIR and (b) Raman spectra of the as-prepared glasses.

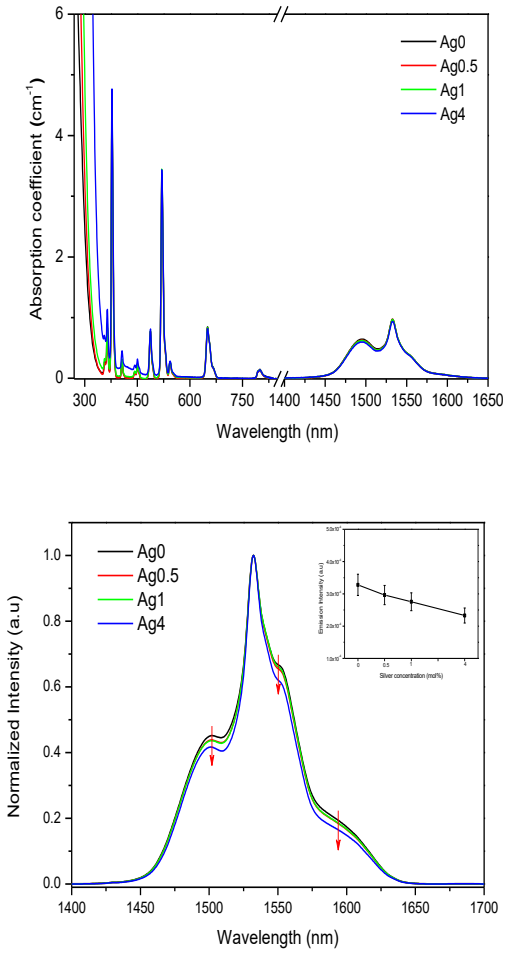

Fig. 3: (a) Absorption and (b) normalized Near-IR emission spectra of the as-prepared glasses (λ_{exc}=980nm). The inset (b) shows the intensity of the emission versus the Ag concentration.

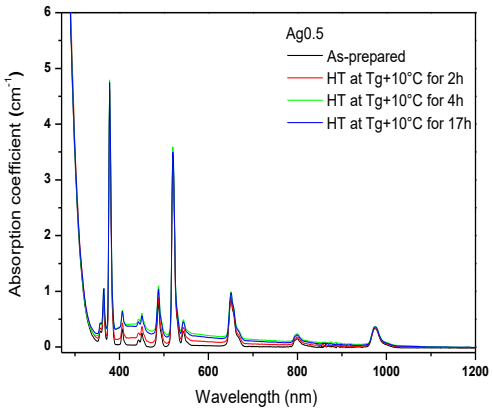

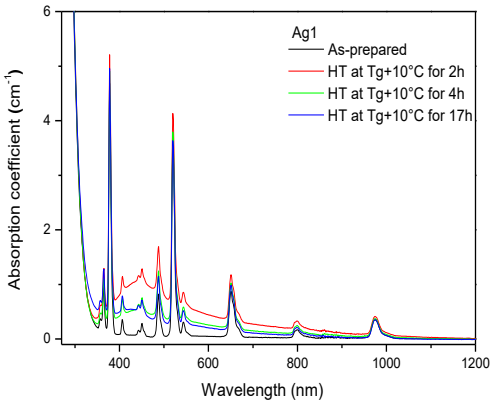

(a) **(b)**

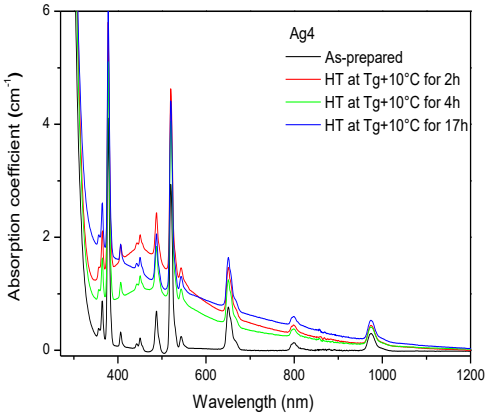

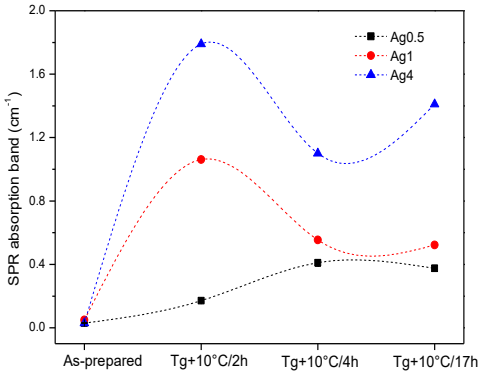

(b) **(d)**

Fig. 4: Absorption spectra of the Ag-containing glasses prior to and after heat-treatment at T_g*+10 °C* for 2, 4, and 17h.

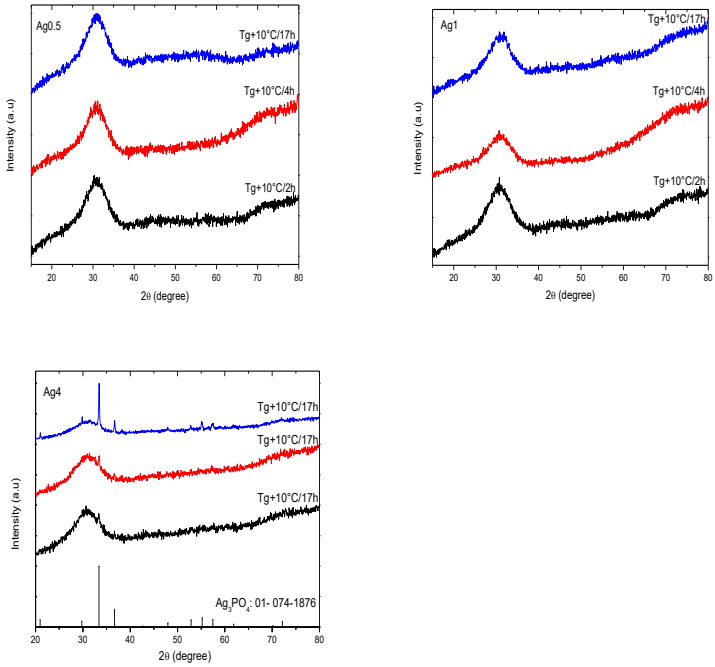

(a) **(b)** **(c)**

Fig. 5 : X-ray diffraction patterns of Ag0.5 (a), Ag1 (b), and Ag4 (c) glasses heat-treated at T_g+*10°C* for 2, 4, and 17h.

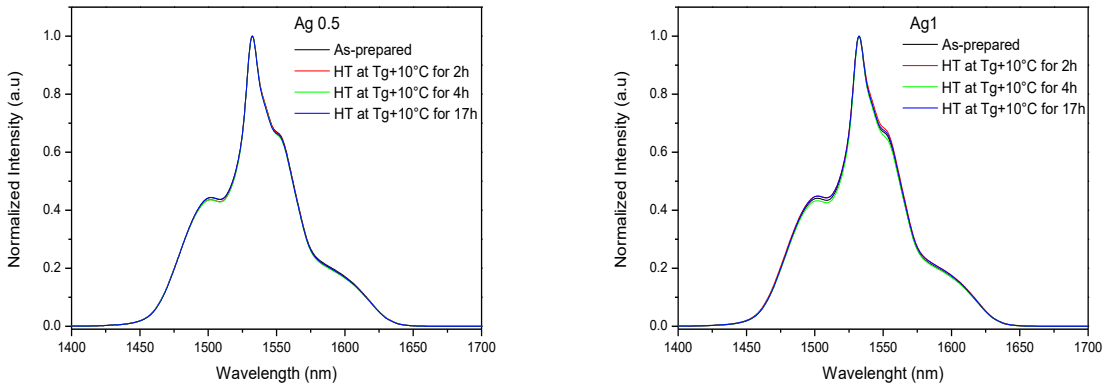

(a) (b)

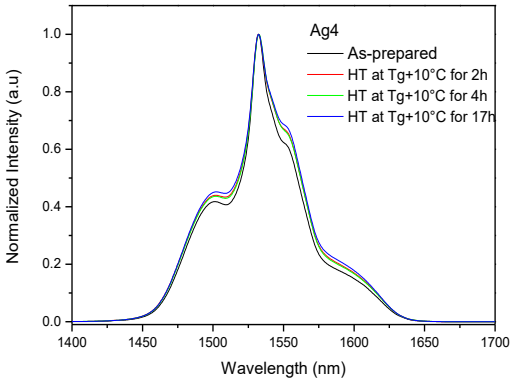

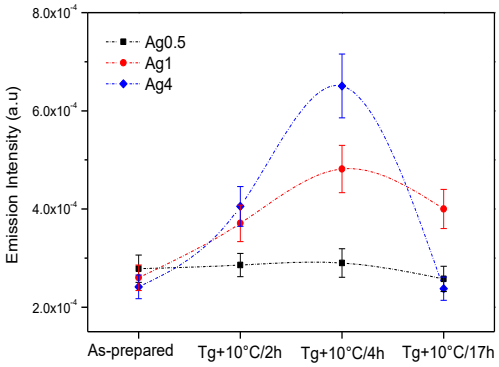

(c) (d)

Fig. 6 : Emission spectra at 1.53 µm of the glasses prior to and after heat-treatment at T_g+*10°C*, under excitation of 980 nm.

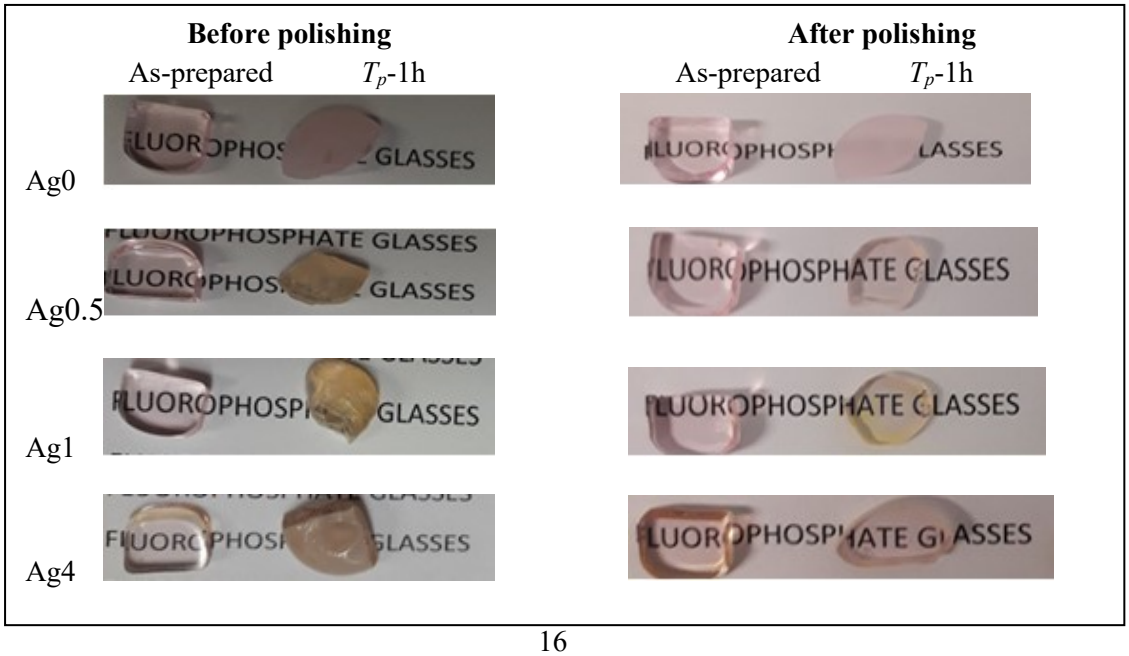

Fig. 7: Picture of the glasses heat-treated at T_g+*20°C* for 17 h, then at T_p for 1h prior to and after polishing.

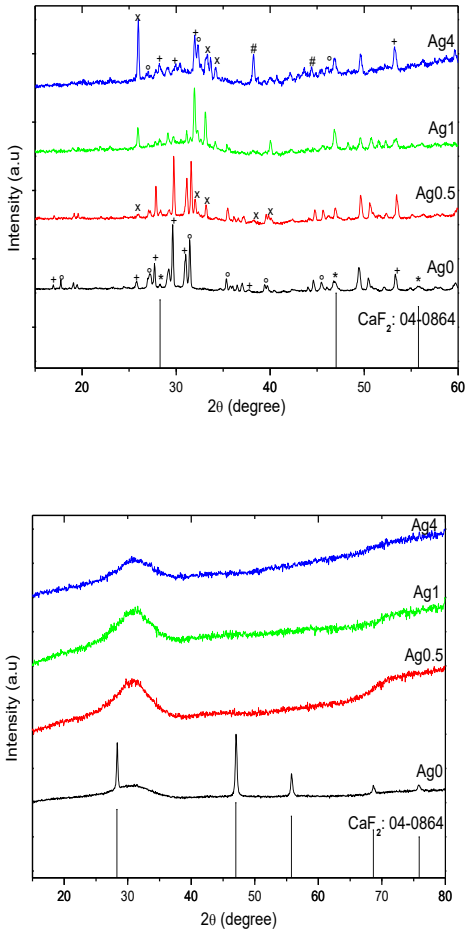

(a) **(b)**

Fig. 8: XRD patterns of the investigated glasses heat-treated at T_g+*20°C* for 17 h, then at T_p for 1h prior to (a) and after (b) polishing, the diffraction peaks are linked to $^{*}CaF_2$, $^{+}Ca(PO_3)_2$, $^{\circ}Ca_3(PO_4)_2$, $^{x}Ca_5(PO_4)_3F$ and $^{\#}Ag$.

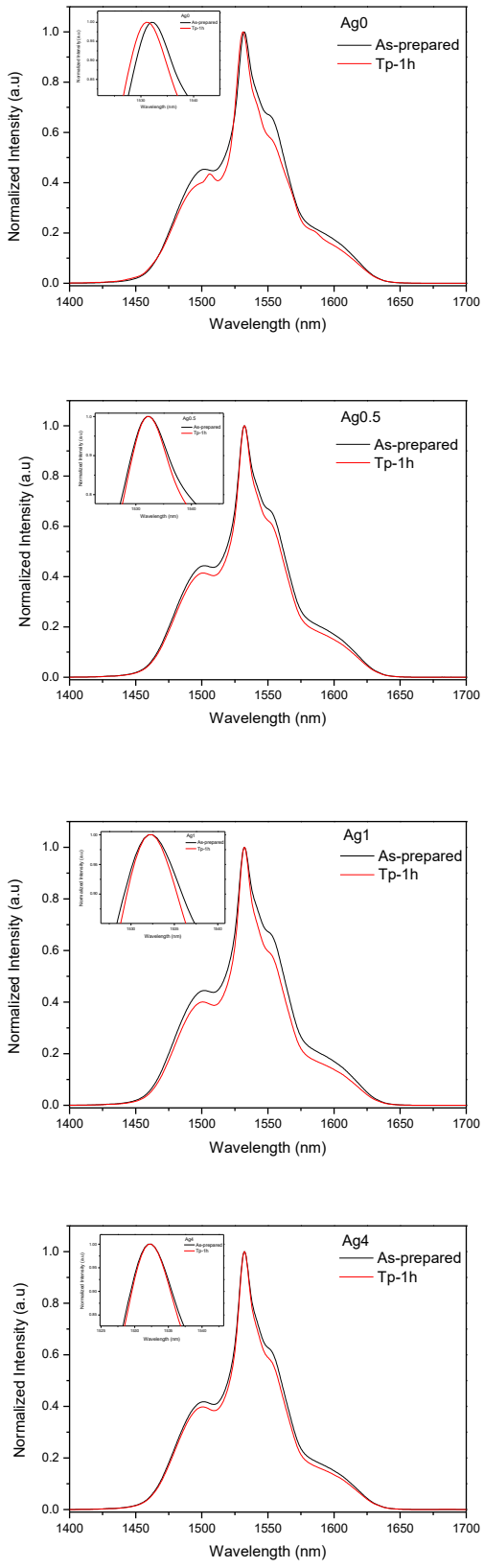

Fig. 9: Normalized emission spectra at 1.53 µm of the glasses before and after heat-treatment at T_g+20°C, followed by a hold at their T_p for 1h